Measurement of the neutron capture cross-section of ^{238}U at neutron energies of 5.9 ± 0.5 and 15.5 ± 0.7 MeV by using the neutron activation technique

CrossMark

V.K. Mulik [a], S.V. Surayanarayana [b], H. Naik [c,*], Sadhana Mukerji [d], B.S. Shivashankar [e], P.M. Prajapati [f], S.D. Dhole [a], V.N. Bhoraskar [a], S. Ganesan [d], A. Goswami [c]

[a] Department of Physics, University of Pune, Pune 411 007, India
[b] Nuclear Physics Division, Bhabha Atomic Research Centre, Mumbai 400 085, India
[c] Radiochemistry Division, Bhabha Atomic Research Centre, Mumbai 400 085, India
[d] Reactor Physics Design Division, Bhabha Atomic Research Centre, Mumbai 400 085, India
[e] Department of Statistics, Manipal University, Manipal 576 104, India
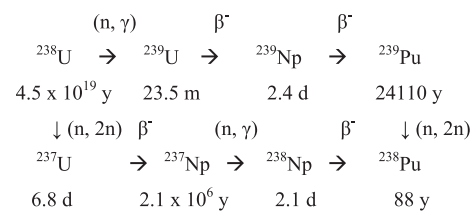[f] Physics Department, Faculty of Science, The M.S. University of Baroda, Vadodara 390 002, India

ARTICLE INFO

ABSTRACT

The ^{238}U(n, γ)^{239}U reaction cross-sections at average neutron energies of 5.9 ± 0.5 and 15.5 ± 0.7 MeV from the ^{7}Li(p, n) reaction have been determined using neutron activation and off-line γ-ray spectrometric technique. The ^{238}U(n, 2n)^{237}U reaction cross-section at neutron energy of 15.5 ± 0.7 MeV has also been determined using the same technique. The ^{238}U(n, γ)^{239}U and ^{238}U(n, 2n)^{237}U reaction cross-sections have been calculated theoretically using nuclear reaction model based TALYS-1.4 code and are found to be in general agreement with measured experimental data. The present data are compared with the values from the latest available evaluated nuclear data libraries and found to be agreement with the data of ENDF/B-VII.1, JENDL-4.0 and JEFF-3.1/A but not with that of CENDL-3.1.

© 2013 Elsevier Ltd. All rights reserved.

1. Introduction

The ^{238}U(n, γ)^{239}U and ^{238}U(n, 2n)^{237}U reaction cross-sections are of primary importance from the reactor point of view. This is because most of the reactors presently operating in the world are light water reactors (PWR and BWR) or heavy water reactors (HWR), which are based on enriched or natural uranium as a fuel. In recent times, significant effort has been made to develop the fast reactor to fulfill the increased demand of power production, for example, see IAEA-TECDOC, 2002; MacDonald and Todreas, 2000; Mathieu et al., 2005; Nuttin et al., 2005; Allen and Crawford, 2007. In a fast reactor, ^{238}U–^{239}Pu in the form of carbide is used as the primary fuel. The fast reactor has a neutron spectrum from 0.1 keV to 15 MeV, and therefore, the production of long-lived minor actinides can be suppressed. The ^{239}Pu used in the fast reactor is first generated in a research reactor from the ^{238}U(n, γ)^{239}U reaction followed by successive two beta decays. Besides this, other reaction products such as long-lived minor actinides (e.g. ^{237}Np,

^{240}Pu, ^{241}Am, ^{243}Am and ^{244}Cm) forms through (n, γ) and (n, 2n) reactions of ^{238}U and ^{239}Pu followed by successive beta decays. A schematic diagram of the ^{238}U(n, γ) and ^{238}U(n, 2n) reactions to produce ^{239}Pu and ^{237}Np in a reactor is shown below.

$$
\begin{array}{ccccccc}
& (n, \gamma) & & \beta^- & & \beta^- & \\
^{238}U & \rightarrow & ^{239}U & \rightarrow & ^{239}Np & \rightarrow & ^{239}Pu \\
4.5 \times 10^{19}\,y & & 23.5\,m & & 2.4\,d & & 24110\,y \\
\downarrow (n, 2n) & \beta^- & & (n, \gamma) & & \beta^- & \downarrow (n, 2n) \\
^{237}U & \rightarrow & ^{237}Np & \rightarrow & ^{238}Np & \rightarrow & ^{238}Pu \\
6.8\,d & & 2.1 \times 10^6\,y & & 2.1\,d & & 88\,y
\end{array}
$$

From the above schematic diagram, it can be seen that the ^{238}U(n, γ)^{239}U and ^{238}U(n, 2n)^{237}U are the primary reactions followed by beta decay to produce long-lived actinides such as ^{239}Pu and ^{237}Np. This is because the neutron spectrum in a conventional reactor varies within 0–15 MeV, whereas in a fast reactor it is within 0.1–15 MeV. In the fast breeder reactor, ^{238}U is used as

---

* Corresponding author. Tel.: +91 22 25594569; fax: +91 22 25505151.
  E-mail address: naikhbarc@yahoo.com (H. Naik).

the breeding material to regenerate the fissile material ^{239}Pu. Thus, the production of fissile material ^{239}Pu depends on the ^{238}U(n, γ)^{239}U reaction cross-section, which is required with an accuracy of 1–2% for predicting the dynamical behavior of the complex arrangements in the fast reactor (Pronyaev, 1999; Kuz'minov and Manokhin, 1997). In fusion–fission hybrid systems, a sensitivity study has shown that the production rate of ^{239}Pu can be predicted within 1%, provided that the ^{238}U(n, γ)^{239}U cross-section between 3 keV and 3 MeV is known within 2% (Cheng and Mathews, 1979). In the fast breeder reactors, the most important region for neutron capture of ^{238}U lies between 10 keV to 100 keV (Bartine, 1979). At neutron energy of 7 eV, the ^{238}U(n, γ)^{239}U reaction cross-section shows a sharp increasing trend due to resonance neutron capture. Then the resolved resonance region extends up to 20 keV. Thereafter it decreases up to neutron energy of 6–7 MeV, where the ^{238}U(n, 2n)^{237}U reaction cross-section starts. The threshold energy of the ^{238}U(n, 2n)^{237}U reaction cross-section is 6.18 MeV. Thus, above the neutron energy of 6.18 MeV, the ^{238}U(n, 2n)^{237}U reaction is one of the channel besides (n, f) and (n, γ) reactions of ^{238}U. Above neutron energy of 6.18 MeV, the ^{238}U(n, 2n)^{237}U reaction cross-section increases rapidly with neutron energy. Thus, the ^{238}U(n, γ)^{239}U and ^{238}U(n, 2n)^{237}U reactions cross-sections at higher neutron energy have a strong impact on the performance and safety assessment for fast reactor (Pelloni et al., 1997). This is because the neutron economy in a reactor is affected by the above reactions. Hence, it is important to measure the ^{238}U(n, γ)^{239}U and ^{238}U(n, 2n)^{237}U reactions cross-sections at different neutron energies.

The ^{238}U(n, γ)^{239}U reaction cross-section is available in the literature over a wide range of neutron energies from thermal to 20 MeV based on physical measurements (Batchelor et al., 1965; Asghar et al., 1966; Menlove and Poenitz, 1968; Drake et al., 1971; de Saussure et al., 1973; Poenitz, 1975; Liou and Chrien, 1977; Wisshak and Kappeler, 1978; Perez et al., 1979; Mc Daniels et al., 1982; Voignier et al., 1992) and activation techniques (Leipunskiy et al., 1958; Hann and Rose, 1959; Panitkin and Tolstikov, 1972a,b; Panitkin and Sherman, 1975; Lindner et al., 1976; Poenitz et al., 1981; Buleeva et al., 1988; Quang and Knoll, 1992; Naik et al., 2012). Similarly, ^{238}U(n, 2n)^{237}U reaction cross-section data is also available in a wide range of neutron energies above 6 MeV from off-line γ-ray spectrometry and neutron activation method (Naik et al., 2012; Landrum et al., 1973; Karius et al., 1979; Kornilov et al., 1980; Frchaut et al., 1980; Shani, 1983; Wang et al., 2010). Besides the experimental data in IAEA-EXFOR, evaluated data of ^{238}U(n, γ)^{239}U and ^{238}U(n, 2n)^{237}U reactions cross-sections over a wide range of neutron energies are available from different compilations such as ENDF/B-VII.1 (Chadwick et al., 2011), JENDL-4.0 (Shibata et al., 2011), JEFF-3.1/A (Koning et al., 2007), CENDL-3.1 (Ge et al., 2011) and Da-Zhao and Tai-Chang (1978).

From the above literature data (IAEA-EXFOR), it can be seen that the ^{238}U(n, γ)^{239}U reaction has numerous resonances cross-section from the neutron energy of 7 eV to 20 keV. However, above neutron energy of 20 keV the ^{238}U(n, γ)^{239}U reaction cross-section decreases up to 6–7 MeV (Panitkin and Tolstikov, 1972a,b; Lindner et al., 1976; Poenitz et al., 1981; Buleeva et al., 1988; Naik et al., 2012). The ^{238}U(n, γ)^{239}U reaction cross-section data from our earlier work (Naik et al., 2012) at 3.7 MeV is in agreement with the data of Leipunskiy et al. (1958) and Panitkin and Tolstikov (1972a,b). Above neutron energy of 7 MeV, the ^{238}U(n, γ)^{239}U reaction cross-section data of Mc Daniels et al. (1982) decreases sharply and remains almost constant up to 14 MeV. At neutron energy of 9.85 MeV, our earlier data (Naik et al., 2012) is comparable to the data of Mc Daniels et al. (1982). At neutron energy of 17 MeV, the ^{238}U(n,γ)^{239}U reaction cross-section data of Panitkin and Tolstikov (1972a,b) increase suddenly compared to the data of Mc Daniels et al. (1982) and thereafter remain constant up to 20 MeV. Thus, the data of Leipunskiy et al. (1958) and Panitkin and Tolstikov (1972a,b) above neutron energy of 3.7 MeV and the data of Panitkin and Tolstikov (1972a,b) above 17 MeV are higher than the evaluated data from ENDF/B-VII.1, JENDL-4.0, JEFF-3.1/A. On the other hand, our earlier data at neutron energy of 9.85 MeV (Naik et al., 2012) and the data of Mc Daniels et al. (1982) within 7–14 MeV are in agreement with the evaluated data of ENDF/B-VII.1, JENDL-4.0 and JEFF-3.1/A compilation. Further, there is a mismatch between the ^{238}U(n, γ)^{239}U reaction cross-section data between the experiment (IAEA-EXFOR) and evaluation (Chadwick et al., 2011; Shibata et al., 2011; Koning et al., 2007; Ge et al., 2011). From the above observations it is clear that there are three different trends of ^{238}U(n, γ)^{239}U reaction cross-section within the neutron energy of 0.1–20 MeV. However, the evaluated data from CENDL-3.1 are in agreement with the experimental data over wide range of neutron energies but have entirely different trend than the evaluated data of ENDF/B-VII.1, JENDL-4.0 and JEFF-3.1/A compilations. Similarly, the Da-Zhao and Tai-Chang (1978) also shows a different trend than the evaluated data of ENDF/B-VII.1, JENDL-4.0 and JEFF-3.1/A compilations. Thus, it is necessary to determine the ^{238}U(n, γ)^{239}U reaction cross-section experimentally within neutron energies of 3.7–7.0 MeV and 14–20 MeV.

Above neutron energy of 6.18 MeV, the ^{238}U(n, 2n)^{237}U reaction become the pre-dominant mode besides the (n, γ) and (n, f) reactions of ^{238}U. It can be seen from the literature data of Naik et al. (2012), Landrum et al. (1973), Kairus et al. (1979), Kornilov et al. (1980), Frchaut et al. (1980), Shani (1983), Wang et al. (2010) that the increase of ^{238}U(n, 2n)^{237}U reaction cross-section is very sharp from the neutron energy of 6.18 MeV to 7–8 MeV and then remains constant up to 13–14 MeV. Thereafter, it decreases with increase of neutron energy due to opening of other reaction channels such as (n, 2nf) and (n, xn). The available experimental ^{238}U(n, 2n)^{237}U reaction cross-section at different neutron energy (Naik et al., 2012; Landrum et al., 1973; Karius et al., 1979; Kornilov et al., 1980; Frchaut et al., 1980 ; Shani, 1983; Wang et al., 2010) is in close agreement with the evaluated data of ENDF/B-VII.1, JENDL-4.0 and JEFF-3.1/A compilations and follows a smooth trend.

In spite of the availability of sufficient data in literature (IAEA-EXFOR), the need for accurate re-measurement arises in order to examine the discrepancies of the available experimental data and various evaluations. In view of this, in the present work we have determined the ^{238}U(n, γ)^{239}U and ^{238}U(n, 2n)^{237}U reaction cross-sections at average neutron energies of 5.9 ± 0.5 and 15.5 ± 0.7 MeV. The experiment was carried out using neutron activation method followed by off-line γ-ray spectrometry, and the neutrons are generated from ^{7}Li(p, n) reaction. The ^{238}U(n, γ) and ^{238}U(n, 2n) reaction cross-sections were also calculated theoretically using nuclear reaction model based TALYS-1.4 computer code and compared with the experimental data.

2. Experimental

The present experiment has been carried out at the 14UD BARC-TIFR Pelletron accelerator facility at Mumbai, India. The neutron beam was generated using the ^{7}Li(p, n) reaction from the proton beam main line at 6 m above the analyzing magnet of the Pelletron facility to utilize the maximum proton current from the accelerator. The proton energies of the experiment were 7.8 and 18 MeV, respectively. A collimator of 6 mm diameter made of graphite was used before the Li target to avoid the spatial spread of the proton beam. The energy spread for proton beam at 6 m height was maximum 50–90 keV. At this port, the terminal voltage was regulated by GVM mode using a terminal potential stabilizer. The lithium foil used for neutron production was made up of natural

lithium foil with thickness of 3.713 mg/cm². The uncertainty in the thickness of lithium foil was about 0.025 mg/cm². Usually lithium foil is stored inside kerosene or silicon oil because in air it oxides immediately and catches fire in presence of moisture. Before use only it was removed from kerosene, dried and rolled up of desired thickness. The lithium foil was sandwiched between two tantalum foils of different thickness. The front thin tantalum foil facing the proton beam has a thickness of 3.92 mg/cm², in which degradation of proton energy is only 50–80 keV as calculated from the SRIM computer code (Ziegler et al., 2008). This is based on the uncertainty of 0.02 mg/cm² in thickness of tantalum foil. On the other hand, the back thick tantalum foil has a thickness of 0.025 mm, which is sufficient to stop the proton beam. Behind the Ta–Li–Ta stack, the samples used for neutron irradiation were placed at a distance of 2.05 cm.

The samples consist of natural U metal foil, wrapped with 0.025 mm thick super pure aluminum foil of purity 99.99%. The aluminum wrapper was used as a catcher foil to stop fission products recoiling out from the ^{nat}U metal foil during the irradiation. The size of ^{nat}U metal foil was 1.0 cm² with thickness of 634.2 mg/cm². The uncertainty of the ^{nat}U was about 1.6 mg/cm². The U sample wrapped with aluminum foil was mounted at 0° angles in the forward direction with respect to the incident beam direction at a distance of 2.05 cm from the location of the Ta–Li–Ta stack. The distance of the target to the collimator was only 5 mm. Since the U target was fixed on a screw tide stand, the positional uncertainty from the location of the Ta–Li–Ta stack was 0.5 mm. A schematic diagram of Ta–Li–Ta stack and sample is given in Fig. 1. Different sets of Ta–Li–Ta stacks and U sample wrapped with aluminum foil were made for different irradiations at various neutron energies.

The U sample along with Al wrapper was irradiated by the neutrons generated by impinging the proton beam on the lithium metal foil through the thin tantalum foil of the Ta–Li–Ta metal stack. In the first set, the irradiation time was 15 h for the neutron beam corresponding to the proton beam energy of 7.8 MeV. Similarly, in the second set, the irradiation time was 5 h for the neutron beam corresponding to the proton beam energy of 18 MeV. The proton current during the irradiations varies from 300–400 nA. For the proton energies of 7.8 and 18 MeV, the corresponding average neutron energies faced by U samples were 5.9 and 15.5 MeV, respectively. After irradiation, the samples were cooled for 1–2 h. Then, the irradiated samples of U along with Al wrapper were mounted on different Perspex plates and taken for the γ-ray counting.

The γ-rays of reaction/fission products from the irradiated U sample were counted in energy and efficiency calibrated 80 cm³ HPGe detector coupled to a PC-based 4 K channel analyzer. The resolution of the detector system had a FWHM of 1.8 keV at 1332.5 keV of ^{60}Co. Measurements were done by keeping suitable distance of 2–5 cm between the sample and the end cap of the detector to keep the dead time within 5% and to avoid the pileup eff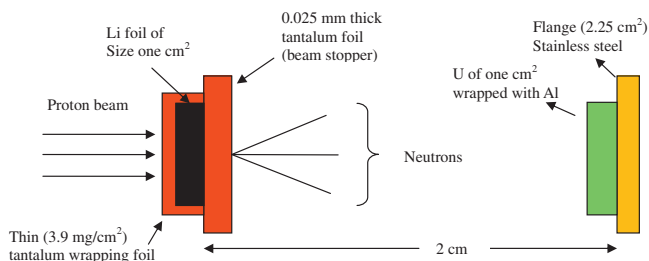ects. The γ-ray counting of the sample was done in live time mode and was followed as a function of time. The energy and efficiency calibration of the detector system was done by counting the γ-ray energies of standard ^{152}Eu and ^{133}Ba sources (Nudat-2.6). The γ-ray counting of the standard sources were done at the same geometry, with negligible summation error. The detector efficiency was 20% at 1332.5 keV relative to 3″ diameter ×3″ length NaI(Tl) detector. The γ-ray counting of the irradiated U samples was done up to few months to check the half-life of the radio nuclides of interest. Fig. 2 shows a typical γ-ray spectrum of the ^{239}Np and ^{237}U from the irradiated U with 15.5 MeV neutrons, in which photo-peak at 106.1 keV of ^{239}Np and 208 keV of ^{237}U are clearly observed.

3. Analysis of the experiment

3.1. Calculation of the neutron energy

In the present experiment, the neutron flux was produced from the ^{7}Li(p, n) reaction at the incident proton energies of 7.8 MeV and 18.0 MeV. The Q-value for the ^{7}Li(p, n)^{7}Be reaction to the ground state is −1.644 MeV, whereas the first excited state is 0.431 MeV above ground state leading to an average Q-value of −1.868 MeV. However, the threshold value to populate the ground state of ^{7}Be is 1.881 MeV. Thus, for the proton energy of 7.8 and 18.0 MeV the resulting peak energy of first group of neutrons (n_0) will be 5.92 and 16.12 MeV, respectively. The corresponding neutron energy of second group of neutrons (n_1), for the first excited state of ^{7}Be will be 5.42 and 15.62 MeV, respectively. The branching ratio to the ground state and first excited state of ^{7}Be up to $E_p = 7$ - MeV is given by Liskien and Paulsen (1975). In addition to these, Meadows and Smith (1972) have also given the branching ratio to the ground state and first excited state of ^{7}Be up to 7 MeV. On the other hand, Poppe et al. (1976) have given the branching ratio to the ground state and first excited state of ^{7}Be for $E_p = 4.2$ MeV to 26 MeV. Above proton energy of 4.5 MeV, the fragmentation of ^{8}Be to ^{4}He + ^{3}He + n ($Q = −3.23$ MeV) occurs and other reaction channel opens to give a continuous neutron energy distribution besides n_0 and n_1 groups of neutrons. Meadows and Smith (1972) have given experimental neutron distributions from the break up channels and also parameterized these distributions. For the proton energies of 7.8 and 18.0 MeV, we have generated the neutron spectrum using the neutron energy distribution given by Poppe et al. (1976) within half-angle of 22°, which are given in Figs. 3 and 4, respectively. This is because for the U metal foil of 5 mm radius
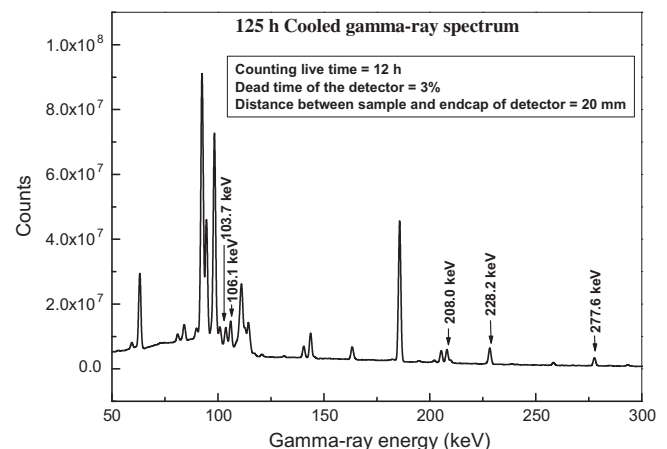

Fig. 1. Schematic diagram showing the experimental set up used for neutron irradiation using ^{7}Li(p, n) reaction. Drawing is not in actual scale.

Fig. 2. Gamma-ray spectrum of ^{239}Np and ^{237}U, respectively produced through ^{238}U(n, γ)^{239}U and ^{238}U(n, 2n)^{237}U reactions induced by 15.5 ± 0.7 MeV neutrons.
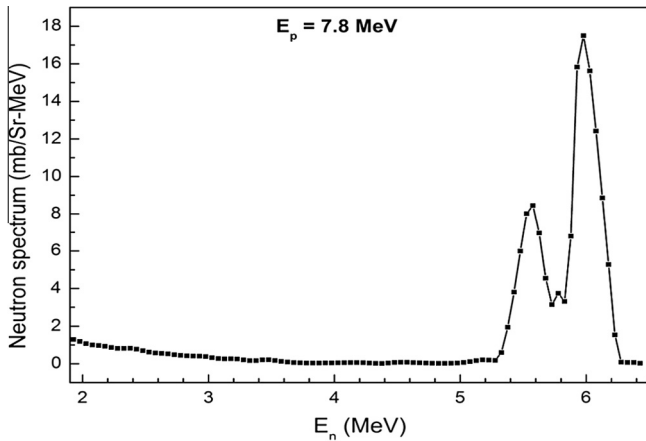
Fig. 3. Neutron spectrum for ^{7}Li(p, n)^{7}Be reaction at E_P = 7.8 MeV within half-angle of 22°, calculated using the results of Poppe et al. (1976).

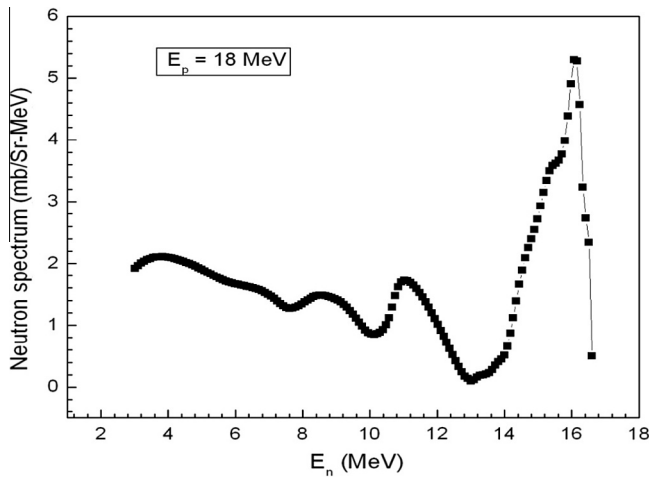**Fig. 4.** Neutron spectrum for ^{7}Li(p, n)^{7}Be reaction at E_P = 18 MeV within half-angle of 22°, calculated using the results of Poppe et al. (1976).

and Li target of 3 mm diameter with 2 cm Li–U distance, the maximum half-angle is 22°. From Figs. 3 and 4, the average neutron energies under the main peak region (n_0 and n_1 groups) were calculated as 5.9 ± 0.4 and 15.5 ± 0.7 MeV, respectively after removing the corresponding tailing regions of the neutron spectrum. The uncertainties are based on the difference of average neutron energy and peak neutron energies of n_0 and n_1 group of neutrons.

3.2. Calculation of the neutron flux

It can be seen from Figs. 3 and 4 that, the tailing region of the low energy neutrons is quite significant. In view of this, neutron flux was calculated using the yield of fission products (^{97}Zr and ^{135}I) in the neutron induced fission of ^{238}U (Nagy et al., 1978; Chapman et al., 1978). This is justified because the yield of fission products (Nagy et al., 1978; Chapman et al., 1978) at peak position of the mass–yield curve does not change significantly. On the other hand the neutron induced fission cross-section of ^{238}U (Blons et al., 1975) changes in a manner of step function with increase of neutron energy. The following equation (Naik et al., 2012) was used for the neutron flux (Φ) calculation.

$$\Phi = \frac{A_{net}(CL/LT)\lambda}{N\sigma_f Ya\varepsilon(1 - e^{-\lambda T})e^{-\lambda T}(1 - e^{-\lambda CL})} \qquad (1)$$

where A_{net} is the net photo-peak area for the 743.36 and 1260.4 keV γ-lines of the fission products ^{97}Zr and ^{135}I, respectively. N is the number of target atoms and σ_f is the average fission cross-section of ^{238}U(n, f) reaction (Blons et al., 1975) at different neutron energies, which is obtained by folding with the neutron spectrum. Y is the yield of the fission product (Nagy et al., 1978; Chapman et al., 1978). 'a' is the branching intensity of the gamma lines and 'ε' is its detection efficiency. 't', T, CL and LT are the irradiation time, cooling time, clock time and counting time, respectively. In the above equation, the 'CL/LT' term has been used for dead time correction, which is same as the value displayed in the analyzer of the multi-channel analyzer system.

The net photo-peak area (A_{net}) of 743.36 keV (^{97}Zr) and 1260.4 keV (^{135}I) γ-lines were obtained by using PHAST peak fitting program (Mukhopadhyaya, 2001). The nuclear spectroscopic data such as half-life and γ-ray intensity were taken from literature (Nudat-2.6). Using the Eq. (1), the neutron flux was obtained to be $(3.53 \pm 0.21) \times 10^6$ n cm^{-2} sec^{-1} for the neutron energy of 5.9 ± 0.5 MeV and $(1.54 \pm 0.08) \times 10^7$ n cm^{-2} sec^{-1} for the neutron energy of 15.5 ± 0.7 MeV, which were used for the ^{238}U(n, γ) reaction cross-sections calculation. The neutron flux for the ^{238}U(n, 2n) reaction at the average neutron energy of 15.5 ± 0.7 MeV was obtained as $(1.05 \pm 0.08) \times 10^7$ n cm^{-2} sec^{-1}. This value was obtained based on the ratio of neutron flux of the neutron spectrum of Fig. 4 for ^{238}U(n, 2n) reaction above its threshold to total flux. There is some attenuation of the γ-ray energy of the fission products and the reaction products inside the U-metal foil are different. However, they were found to be less than 1% due to the 0.025 mm thick U foil. This can change the neutron flux only within the uncertainty limits as mentioned above and are taken care.

3.3. Determination of ^{238}U(n, γ)^{239}U and ^{238}U(n, 2n)^{237}U reaction cross-sections and their results

For the calculation of the ^{238}U(n, γ)^{239}U and ^{238}U(n, 2n)^{237}U reactions cross-sections, the nuclear spectroscopic data (Basunia, 2006; Nudat-2.6) used in the present work are given in Table 1. The ^{238}U(n, γ)^{239}U reaction cross-section can be calculated from the 74.7 keV γ-ray activity of the reaction product ^{239}U. However, the half-life of ^{239}U is only 23.45 min., which decays almost completely to ^{239}Np within 3 h. In view of this, the ^{238}U(n, γ)^{239}U reaction cross-section (σ) was calculated from the γ-ray activity of its daughter product ^{239}Np. Since ^{239}Np have the half-life of 2.35 d, its observed photo-peak activity from the γ-ray spectrum measured after sufficient cooling time was used for the calculation. In the case of ^{238}U(n, 2n)^{237}U reaction, the cross-section was calculated from the γ-ray activity of ^{237}U, obtained from the γ-ray spectrum measured after sufficient cooling time. The equation used for the calculation of cross-sections (σ) (Naik et al., 2012) for the ^{238}U(n, γ) and ^{238}U(n, 2n) reactions is given below.

Table 1
Nuclear data used in this work (Basunia, 2006; Nudat-2.6).

Nuclide	Half life	γ-Ray energy (keV)	γ-Ray abundance (%)
^{97}Zr	16.74 h	743.36	93.1
^{135}I	6.57 h	1260.4	28.7
^{237}U	6.75 d	101.1	24.5
		208.0	21.2
^{239}U	23.45 m	74.7	49.2
^{239}Np	2.35 d	103.4	22.2
		106.1	26.3
		228.2	11.14
		277.6	14.44

$$\sigma = \frac{A_{obs}(CL/LT)\lambda}{Na\varepsilon\Phi(1 - e^{-\lambda T})e^{-\lambda T}(1 - e^{-\lambda CL})} \quad (2)$$

All terms in Eq. (2) have the similar meaning as in the Eq. (1). The experimentally determined ^{238}U(n, γ) reaction cross-sections at the average neutron energies of 5.9 ± 0.5 and 15.5 ± 0.7 MeV are 4.650 ± 0.125 and 2.389 ± 0.075 mb, respectively. Similarly, the experimentally determined ^{238}U(n, 2n) reaction cross-section at an average neutron energy of 15.5 ± 0.7 MeV is 1094 ± 76 mb. There is a possibility of contribution to the reaction cross-sections from the scattered neutrons of the floor, roof and surrounding wall materials. It was estimated before the experiment without U target irradiation and was found to be below detection limit and thus ignored. However, there is some contribution to the ^{238}U(n, γ)^{237}U reaction cross-section from the low energy neutron reaction cross-section. The contribution of the ^{238}U(n, γ) reaction cross-section arises from the tail region of the neutron spectrum of Figs. 3 and 4. This has been estimated by folding the evaluated ENDF/B-VII.1, JENDL-4.0 and JEFF-3.1/A cross-sections with tailing part of the neutron flux distributions of Figs. 3 and 4 (Liskien and Paulsen, 1975; Meadows and Smith, 1972; Poppe et al., 1976). At proton energy of 7.8 MeV, the contribution to the ^{238}U(n, γ) reaction cross-section are obtained as 3.48, 3.56 and 3.43 mb from ENDF/B-VII.1, JENDL-4.0 and JEFF-3.1/A, respectively. Similarly, at proton energy of 18 MeV the contribution to the ^{238}U(n, γ) reaction cross-section are 1.91, 1.48 and 1.91 mb from ENDF/B-VII.1, JENDL-4.0 and JEFF-3.1/A, respectively.

In the case of ^{238}U(n, 2n)^{237}U reaction cross-section, since the neutron spectrum for proton energy of 18 MeV in Fig. 4 has a tailing part, its contribution to the cross-section based on evaluated data of ENDF/B-VII.1, JENDL-4.0 and JEFF-3.1/A are obtained as 565.4, 550.2 and 565.6 mb, respectively. The neutron tail contributions to the ^{238}U(n, γ)^{239}U and ^{238}U(n, 2n)^{237}U reaction cross-sections based on CENDL-3.1 evaluated data are entirely different from others evaluations and thus not mentioned.

After removing the tailing contribution, the actual experimental ^{238}U(n, γ)^{239}U reaction cross-sections obtained at an average neutron energies of 5.9 ± 0.5 and 15.5 ± 0.7 MeV are 1.158 ± 0.125 and 0.623 ± 0.075 mb, respectively. These values are given in Table 2 along with our earlier data (Naik et al., 2012) at other neutron energies. The ^{238}U(n, 2n) reaction cross-section at an average neutron energy of 15.5 ± 0.7 MeV is obtained to be 534 ± 76 mb, which is also given in Table 2 along with our earlier data (Naik et al., 2012) at other neutron energy. Since we have used correction in cross-section based on evaluated data of ENDF/B-VII.1, JENDL-4.0 and JEFF3.1/A, the error due to corrections has been taken into account. The evaluated ^{238}U(n, γ) and ^{238}U(n, 2n) reaction cross-sections from ENDF/B-VII.1, JENDL-4.0 and JEFF-3.1/A are also given in Table 2 for the comparison with our present results.

The uncertainties shown in Table 2 for the ^{238}U(n, γ)^{239}U and ^{238}U(n, 2n)^{237}U reaction cross-sections are based on replicate measurements. This overall uncertainty is the quadratic sum of both statistical and systematic errors. The random error in the observed activity is primarily due to counting statistics, which is estimated to be 4–8%. This can be determined by accumulating the data for an optimum time period that depends on the half-life of nuclides of interest. The systematic errors are due to uncertainties in neutron flux estimation ($\sim$5.2–7.6%), neutron energies weight of U target ($\sim$0.28%), fission cross-section ($\sim$4.2%), the irradiation time ($\sim$0.55%), the energy calibration and efficiency of detector ($\sim$3%), self-absorption of the γ-rays in the sample ($\sim$1%), nuclear decay data such as half-life of the reaction products and the γ-ray abundances ($\sim$2%) based on literature (Basunia, 2006; Nudat-2.6). Thus, the total systematic error is about $\sim$7.7–9.5%. The overall uncertainty is found to range between 8.7 and 12.4%, coming from the combination of a statistical error of 4–8% and a systematic error of 7.7–9.5%.

4. Discussion

The cross-section of ^{238}U(n, γ)^{239}U reaction at $E_n = 5.9 \pm 0.5$ and 15.5 ± 0.7 MeV and of ^{238}U(n, 2n)^{237}U reaction at $E_n = 15.5 \pm 0.7$ MeV of present work are determined using a neutrons from ^{7}Li(p, n) reaction. At $E_n = 15.5 \pm 0.7$ MeV, the ^{238}U(n, γ)^{239}U reaction cross-section is determined for the first time, whereas the ^{238}U(n, 2n)^{237}U reaction cross-section is the re-determined value and is in agreement with the literature data (Karius et al., 1979; Kornilov et al., 1980). At $E_n = 5.9 \pm 0.5$ MeV, the ^{238}U(n, γ)^{239}U reaction cross-section is also re-determined value but is found to be lower than the value of Leipunskiy et al. (1958) and Panitkin and Tolstikov (1972a,b). In order to examine this discrepancy, the experimentally determined ^{238}U(n, γ)^{239}U and ^{238}U(n, 2n)^{237}U reaction cross-sections from the present work were compared with the evaluated data from ENDF/B-VII.1, JENDL-4.0, JEFF-3.1/A and CENDL-3.1 libraries. The evaluated reaction cross-sections of the ^{238}U(n, γ)^{239}U reaction from ENDF/B-VII.1, JENDL-4.0 and JEFF-3.1/A are quoted in Table 2 within the neutron energies of 5.5–6.5 MeV and 15–16 MeV because of the finite width of neutron energy under the main peak of Figs. 3 and 4. For the ^{238}U(n, 2n)^{237}U reaction, the evaluated cross-sections from ENDF/B-VII.1, JENDL-4.0 and JEFF-3.1/A are also quoted in Table 2 within the neutron energy of 15–16 MeV.

It can be seen from the Table 2 that the experimental cross-sections of the ^{238}U(n, γ)^{239}U and ^{238}U(n, 2n)^{237}U reactions of the present work are within the range of evaluated data of ENDF/B-VII.1, JENDL-4.0 and JEFF-3.1/A. However, the evaluated value from CENDL-3.1 data is not in agreement with the present experimental

Table 2
Comparison of the present measured and different evaluated nuclear data values of the cross-sections in the ^{238}U(n, γ) and ^{238}U(n, 2n) reactions at $E_n = 5.9 \pm 0.5$, 15.5 ± 0.7 MeV.

Neutron energy (MeV)	Neutron Flux (n cm^{-2} s^{-1})	Cross-section (mb) Expt.	ENDF/B-VII.1	JENDL-4.0	JEFF-3.1/A
^{238}U(n, γ)^{239}U					
3.7 ± 0.3	$(8.78 \pm 0.38) \times 10^6$	11.6 ± 1.0	11.7–9.45[a]	10.14–5.4[a]	12.67–7.51[a]
5.9 ± 0.5	$(3.53 \pm 0.21) \times 10^6$	1.16 ± 0.13	1.63–1.25[b]	0.92–0.84[b]	1.63–1.27[b]
9.85 ± 0.38	$(1.30 \pm 0.05) \times 10^7$	1.42 ± 0.09	1.05–1.24[c]	1.15–1.00[c]	1.05–1.23[c]
15.5 ± 0.7	$(1.54 \pm 0.08) \times 10^7$	0.62 ± 0.08	0.71–0.58[d]	0.45–0.36[d]	0.71–0.58[d]
^{238}U (n, 2n)^{237}U					
9.85 ± 0.38	$(6.50 \pm 0.25) \times 10^6$	1311 ± 87	1317–1416[c]	1303–1419[c]	1310–1441[c]
15.5 ± 0.7	$(1.05 \pm 0.08) \times 10^7$	534 ± 76	594–423[d]	682–483[d]	590–423[d]

[a] For ^{238}U(n, γ)^{239}U reaction the neutron energy range is 3.3–3.8 MeV.
[b] For ^{238}U(n, γ)^{239}U reaction the neutron energy range is 5.5–6.5 MeV.
[c] For ^{238}U(n, γ)^{239}U and ^{238}U(n, 2n)^{237}U reaction the neutron energy range is 9.0–10.5 MeV.
[d] For ^{238}U(n, γ)^{239}U and ^{238}U(n, 2n)^{237}U reaction the neutron energy range is 15–16 MeV.

value as well as other evaluated data and thus is not quoted in Table 2. In order to examine this aspect, the $^{238}U(n, \gamma)^{239}U$ reaction cross-sections from the present work and similar data from literature given in IAEA-EXFOR are plotted in Fig. 5. The experimental data from our earlier work (Naik et al., 2012) at neutron energies of 3.7 ± 0.3 and 9.85 ± 0.38 MeV are also plotted in the same figure.

It can be seen from Fig. 5 that, the $^{238}U(n, \gamma)^{239}U$ reaction cross-section from our earlier work at E_n = 3.7 ± 0.3 MeV is in agreement with the value of Leipunskiy et al. (1958) and Panitkin and Tolstikov (1972a,b). Similarly, our earlier value at E_n = 9.85 ± 0.38 MeV is also in close agreement with the value of Mc Daniels et al. (1982). However, the present data at E_n = 5.9 ± 0.4 MeV is lower than the value of Leipunskiy et al. (1958) and Panitkin and Tolstikov (1972a,b). The $^{238}U(n, \gamma)^{239}U$ reaction cross-section from present work at 15.5 ± 0.7 MeV is determined for the first time and is not possible to compare with the others data due to its non-availability at near neutron energy in the literature. If the data of Mc Daniels et al. (1982) is extended up to the neutron energy of 15.5 ± 0.7 MeV, then the present value seems to be in agreement with the value of their trend. Similarly, if the data of Panitkin and Tolstikov (1972a,b) is extended to the lower neutron energy side up to 15.5 ± 0.7 MeV, then the present value seems to be lower than the value of their trend. In brief, there is a big discrepancy between the experimental data of Mc Daniels et al. (1982), Leipunskiy et al. (1958), Panitkin and Tolstikov (1972a,b) and the data of present work. The experimental data of Mc Daniels et al. (1982) and of present work has one trend, whereas the data of Leipunskiy et al. (1958), Panitkin and Tolstikov (1972a,b) follows a different trend. In order to examine this, the experimental values based on activation technique as well as the evaluated data from ENDF/B-VII.1, JENDL-4.0, JEFF-3.1/A, CENDL-3.1 libraries and review article of Da-Zhao and Tai-Chang (1978) were plotted in Fig. 5. It can be seen from Fig. 5 that the data of Da-Zhao and Tai-Chang (1978) also shows agreement with the experimental data at lower neutron energy only but not at higher energy. Similarly, the evaluated data of CENDL-3.1 are in agreement with some of the earlier data (IAEA-EXFOR) but not with the present experimental data. However, the overall trend of the evaluated data from CENDL-3.1 is entirely different than the evaluated data from ENDF/B-VII.1, JENDL-4.0 and JEFF-3.1/A. The experimental data of present work at neutron energies of 5.9 ± 0.5 and 15.5 ± 0.7 MeV, earlier work (Naik et al., 2012) at 3.7 ± 0.3 and 9.85 ± 0.38 MeV as well as the data of Mc Daniels et al. (1982) within 7–15 MeV are in good

agreement with the evaluated data of ENDF-B-VII.1, JENDL-4.0 and JEFF-3.1/A. Similarly, the experimental data of Leipunskiy et al. (1958) and Panitkin and Tolstikov (1972a,b) for lower neutron energies show a close agreement with the evaluated data. On the other hand, the experimental data of Leipunskiy et al. (1958) and Panitkin and Tolstikov (1972a,b) at neutron energy of 5–7 MeV and of Panitkin and Tolstikov (1972a,b) within 17–20 MeV are higher than the evaluated data (Chadwick et al., 2011; Shibata et al., 2011; Koning et al., 2007). To examine this discrepancy, the $^{238}U(n, \gamma)^{239}U$ reaction cross-sections are calculated theoretically using nuclear reaction model based TALYS-1.4 computer code (Koning et al., 2012) and plotted in the Fig. 5.

It can be seen from Fig. 5 that t the trend of experimental and evaluated $^{238}U(n, \gamma)^{239}U$ reaction cross-section is well reproduced by TALYS-1.4 computer code. The experimental values of our present work at neutron energies of 5.9 and 15.5 MeV as well as with the values of our earlier work (Naik et al., 2012) and the value of Mc Daniels et al. (1982) within 7–15 MeV are in close agreement with the values from TALYS-1.4 code. On the other hand, the experimental values of Leipunskiy et al. (1958) and Panitkin and Tolstikov (1972a,b) within neutron energies of 5–7 MeV and of Panitkin and Tolstikov (1972a,b) at 17–20 MeV are higher than the theoretical value of TALYS-1.4 code. This is because the experiment carried out by them (Panitkin and Tolstikov, 1972a,b; Poenitz et al., 1981) is based on either D + D or D + T reactions, in which the scattered neutron of lower energy must have contributed to the higher cross-section. Similar thing was observed in the present work due to lower energy neutron tailing from $^7Li(p, n)$ reaction. Thus, the contribution in the $^{238}U(n, \gamma)^{239}U$ reaction cross-section due to the low energy neutrons has been corrected in the present work, which has been mentioned earlier in the calculation. Further, it can be seen from Fig. 5 that the experimental (IAEA-EXFOR), evaluated (Chadwick et al., 2011; Shibata et al., 2011; Koning et al., 2007; Ge et al., 2011) and the theoretical (Koning et al., 2012) $^{238}U(n, \gamma)^{239}U$ reaction cross-section shows a general decrease trend from lower energy up to 7 MeV. However, it shows a dip around the neutron energy of 6–8 MeV, which may be due to the opening of (n, 2n) reaction channel. Beyond 8 MeV, it increases up to neutron energy of 14 MeV and then again decreases due to opening of other reaction channels. In view of this, the $^{238}U(n, 2n)^{237}U$ reaction cross-section from the present work and from literature (Naik et al., 2012; Landrum et al., 1973; Karius et al., 1979; Kornilov et al., 1980; Frchaut et al., 1980; Shani, 1983; Wang et al., 2010) given
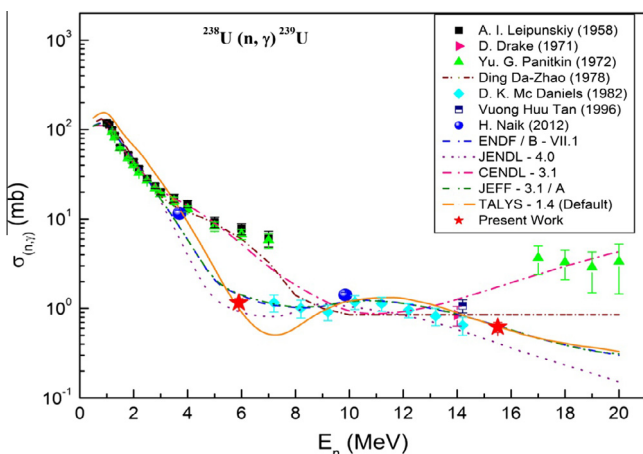

Fig. 5. Plot of experimental and evaluated $^{238}U(n, \gamma)^{239}U$ reaction cross-section as a function of neutron energy from 1 keV to 20 MeV. Experimental values from present work and from IAEA-EXFOR are in different symbols, whereas the evaluated and theoretical values from TALYS-1.4 code are in solid line with different colors.
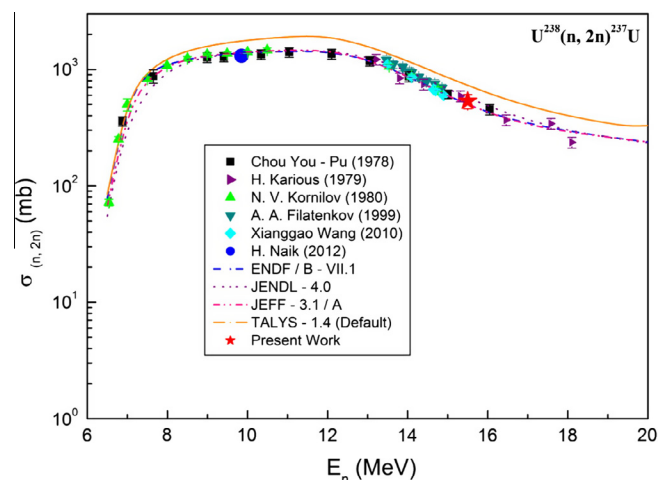
Fig. 6. Plot of experimental and evaluated $^{238}U(n, 2n)^{237}U$ reaction cross-section as a function of neutron energy from 6 MeV to 20 MeV. Experimental values from present work and from IAEA-EXFOR are in different symbols, whereas the evaluated and theoretical values from TALYS-1.4 code are in solid lines with different colors.

in IAEA-EXFOR are plotted in Fig. 6 along with the evaluated data. The ^{238}U(n, 2n)^{237}U reaction cross-sections as a function of incident neutron energy were also calculated theoretically using TALYS-1.4 computer code and plotted in Fig. 6.

It can be seen from Fig. 6 that the ^{238}U(n, 2n)^{237}U reaction cross-section from TALYS-1.4 code are higher than the experimental data of present work and literature data. However, the theoretical ^{238}U(n, 2n)^{237}U reaction cross-section from TALYS-1.4 code shows a similar trend of experimental data. Further, Fig. 6 shows that the experimental and theoretical ^{238}U(n, 2n)^{237}U reaction cross-section shows a sharp increasing trend from the reaction threshold of 6.18 MeV to 8 MeV and there after it remains nearly constant up to 14 MeV. The near constant value of ^{238}U(n, 2n)^{237}U reaction cross-section (Fig. 6) within neutron energy of 8 to 14 MeV is most probably due to the increasing trend of ^{238}U(n, γ)^{239}U reaction cross-section (Fig. 5). Above the neutron energy of 14 MeV, both ^{238}U(n, γ)^{239}U and ^{238}U(n, 2n)^{237}U reaction cross-sections decreases due to opening of other reaction channels.

5. Conclusions

(i) The ^{238}U(n, γ)^{239}U reaction cross-section at average neutron energies of 5.9 ± 0.5 MeV and 15.5 ± 0.7 MeV as well as the ^{238}U(n, 2n)^{237}U reaction cross-section at 15.5 ± 0.7 MeV are determined by off-line γ-ray spectrometric technique and using a neutron source from ^{7}Li(p, n) reaction.

(ii) The ^{238}U(n, γ)^{239}U reaction cross-section at average neutron energies of 5.9 ± 0.5 MeV and 15.5 ± 0.7 MeV and the ^{238}U(n, 2n)^{237}U reaction cross-section at 15.5 ± 0.7 MeV are in general agreement with the evaluated data from ENDF/B-VII.1, JENDL-4.0 and JEFF-3.1/A but with that of CENDL-3.1.

(iii) The ^{238}U(n, γ)^{239}U and ^{238}U(n, 2n)^{237}U reaction cross-sections were calculated theoretically using nuclear model based TALYS-1.4 computer code. The theoretical ^{238}U(n, γ)^{239}U cross-section from TALYS was found to in general agreement with the experimental data of the present work. However, for ^{238}U(n, 2n)^{237}U reaction cross-sections, theoretical values from TALYS are higher than the experimental data.

References

Allen, T.R., Crawford, D.C., 2007. Lead-cooled fast reactor systems and the fuels and materials challenges. Sci. Technol. Nucl. Install. (Article ID 97486).

Asghar, M., Chaffey, C.M., Moxon, M.C., 1966. Low-energy neutron resonance parameters of ^{238}U. Nucl. Phys. 85 (2), 305–316.

Bartine, D.E., 1979. The use of thorium in fast breeder reactors. In: Proceedings of International Conference Nuclear Cross Sections for Technology. NBS-SP 594. National Bureau of Standards, Knoxville, Tennessee, pp. 119.

Basunia, M.S., 2006. Nucl. Data Sheets 107, 3323.

Batchelor, R., Gilboy, W.B., Jowle, J.H., 1965. Neutron interactions with U^{238} and Th^{232} in the energy region 1.6 MeV to 7 MeV. Nucl. Phys. 65, 236–256.

Blons, J., Mazur, C., Paya, D., 1975. Evidence for rotational bands near the ^{232}Th(n, f) fission threshold. Phys. Rev. Lett. 35, 1749–1751.

Buleeva, N.N., Davletshin, A.N., Tipunkov, O.A., Tikhonov, S.V., Tolstokov, V.A., 1988. Neutron radiation capture cross-sections for U-236, U-238, Np-237 measured by the activation method. Atom. Energia 65 (6), 348.

Chadwick, M.B. et al., 2011. ENDF/B-VII.1: nuclear data for science and technology: cross sections, covariances, fission product yields and decay data. Nucl. Data Sheets 112, 2887–2996.

Chapman, T.C., Anzelon, G.A., Spitale, G.C., Nethaway, D.R., 1978. Fission product yields from 6–9 MeV neutron-induced fission of 235U and 238U. Phys. Rev. C 17 (3), 1089–1097.

Cheng, E.T., Mathews, D.R., 1979. The influence of nuclear data uncertainties on thorium fusion-fission hybrid blanket nucleonic performance. In: Proceedings of International Conference on Nuclear Cross Sections for Technology, NBS-SP 594. National Bureau of Standards, Knoxville, Tennessee, pp. 834.

Da-Zhao Ding, Tai-Chang Guo., 1978. Review of U-238 radiative capture cross-Section E_n =1 keV to 20 MeV. Inst. of Atomic Energy, HSJ-77106, China.

de Saussure G., Silver E.G., Perez R.B., Ingle R., Weaver H.,1973. Measurement of the Uranium-238 capture cross section for incident neutron energies up to 100 keV. Nucl. Sci. Eng. 51, 385.

Drake, D., Bergqvist, I., McDaniels, D.K., 1971. Dependence of 14 MeV radiative neutron capture on mass number. Phys. Lett. B 36 (6), 557–559.

Frchaut, J., Bertin, A., Bois, R., 1980. Measurement of the ^{235}U(n, 2n) cross section between threshold and 13 MeV. Nucl. Sci. Eng. 74, 29.

Ge, Z.G. et al., 2011. CENDL-3.1: the updated version of Chinese evaluated nuclear data library. J. Korean Phys. Soc. 59 (2), 1052–1056.

Hann, R.C., Rose, B., 1959. Fast neutron capture in ^{238}U and ^{232}Th. J. Nucl. Energy 8, 197–205.

IAEA-EXFOR Database, <http://www-nds.iaea.org/exfor>.

IAEA-TECDOC, 2002. Fast reactors and accelerator driven systems knowledge base, IAEA-TECDOC-1319: Thorium Fuel Utilization: Options and Trends.

Karius, H., Ackermann, A., Scobel, W., 1979. The pre-equilibrium contribution to the (n, 2n) reactions of ^{232}Th and ^{238}U. J. Phys. G 5, 715.

Koning A.J. et al., 2007. The JEFF evaluated nuclear data project. In: Proceeding of the International Conference on Nuclear Data for Science and Technology, p. 721, Nice, France.

Koning, A.J., Rochman, D., 2012. Modern nuclear data evaluation with the TALYS code system. Nucl. Data Sheets 113, 2841.

Kornilov, N.V., Zhuravlev, B.V., Salnikov, O.A., Raics, P., Nad, Sh., Darotsi, Sh., Sailer, K., Chikai, I., 1980. Measurement of the ^{238}U(n, 2n)^{237}U Cross section in the neutron energy range 6.5-10.5 MeV. Atom. Energy 49, 283.

Kuz'minov, B.D., Manokhin, V.N., 1997. Status of nuclear data for the thorium fuel cycle. Nucl. Const. 3–4, 41.

Landrum, J.H., Nagle, R.J., Lindner, M., 1973. (n, 2n) Cross sections for ^{238}U and ^{237}Np in the region of 14 MeV. Phys. Rev. C 8, 1938–1944.

Leipunskiy A.I., Kazachkovskiy O.D., Artyukhov G. Ja., Baryshnikov A.I., Belanova T.S., Galkov V.I., Stavisskiy Yu. Ja., Stumbur E.A., Sherman L.E., 1958. Radiative capture cross-section measurements for fast neutrons. Second International At. En. Conf. 58GENEVA 15, 50.

Lindner, M., Nagle, R.J., Landrum, J.H., 1976. Neutron capture cross sections from 0.1 to 3 MeV by activation measurements. Nucl. Sci. Eng. 59 (4), 381–394.

Liou, H.L., Chrien, R.E., 1977. Epithermal neutron capture in uranium-238. Nucl. Sci. Eng. 62, 463–478.

Liskien, H., Paulsen, A., 1975. Neutron production cross sections and energies for the reactions ^{7}Li(p, n)^{7}Be and ^{7}Li(p, n)^{7}Be* (431 keV). At. Data Nucl. Data Tables 15, 57–84.

MacDonald, P.E., Todreas, N., 2000. Annual Project Status Report. MIT-ANP-PR -071, INEFL/EXT-2009-00994.

Mathieu L., et al., 2005. Proportion for a very simple thorium molten salt reactor. In: Proceedings of Global International Conference, Paper No. 428, Tsukuba, Japan.

Mc Daniels, D.K., Varghese, P., Drake, D.M., Arthur, F., Lindholm, A., Berquist, I., Krumlinde, J., 1982. Radiative capture of fast neutrons by ^{165}Ho and ^{238}U. Nucl. Phys. A 384, 88.

Meadows J.W., Smith D.L., 1972. Neutrons from proton bombardment of natural Lithium. Argonne National Laboratory, Report. ANL-7983.

Menlove, H.O., Poenitz, W.P., 1968. Absolute radiative capture cross section for fast neutrons in ^{238}U. Nucl. Sci. Eng. 33, 24–30.

Mukhopadhyaya P.K., 2001. Personal Communication.

Nagy, S., Flynn, K.F., Gindler, J.E., Meadows, J.W., Glendenin, L.E., 1978. Mass distributions in monoenergetic-neutron-induced fission of ^{238}U. Phys. Rev. C 17 (1), 163–171.

Naik, H., Suryanarayana, S.V., Mulik, V.K., Prajapati, P.M., Shivashankar, B.S., Jagadeesan, K.C., Thakare, S.V., Raj, D., Sharma, S.C., Bhagwat, P.V., Dhole, S.D., Ganesan, S., Bhoraskar, V.N., Goswami, A., 2012. Measurement of the neutron capture cross-section of ^{238}U using the neutron activation technique. J. Radianal. Nucl. Chem. 293 (2), 469–478.

Nudat-2.6, Nuclear decay data. <http://www.nndc.bnl.gov/nudat2/>.

Nuttin, A., Heuer, D., Billebaud, A., Brissot, R., Le Brun, C., Liatard, E., Loiseaux, J.M., Mathieu, L., Meplan, O., Merle-Lucotte, E., Nifenecker, H., Perdu, F., David, S., 2005. Potential of thorium molten salt reactors detailed calculations and concept evolution with a view to large scale energy production. Proc. Nucl. Ener. 46, 77–99.

Panitkin, Yu.G., Sherman, L.E., 1975. Absolute measurements of neutron radiative capture cross-section with energy 30 keV for U-238. Atom. Energia 39, 17.

Panitkin, Yu.G., Tolstikov, V.A., 1972a. Radiative capture of neutrons by U-238 in the neutron energy range 2–4 MeV. Atom. Energia 33, 782.

Panitkin, Yu.G., Tolstikov, V.A., 1972b. Radiative capture of neutrons by U-238 in the neutron energy range 5–20 MeV. Atom. Energia 33, 825.

Pelloni S., Youinou G., Wydler P., 1997. Impact of different nuclear data on the performance of fast spectrum based on the thorium–uranium fuel cycle. In:

Proceedings of International Conference on Nuclear data for Science and Technology, Part II, p. 1172, Trieste, Italy.

Perez, R.B., de Saussure, G., Macklin, R.L., Halperin, J., 1979. Statistical tests for the detection of intermediate structure: Application to the structure of the ^{238}U neutron capture cross section between 5 keV and 0.1 MeV. Phys. Rev. C 20 (2), 528–545.

Poenitz, W.P., 1975. Measurements of the neutron capture cross sections of Gold-197 and Uranium-238 between 20 and 3500 keV. Nucl. Sci. Eng. 57, 300.

Poenitz, W.P., Fawcett Jr., L.R., Smith, D.L., 1981. Measurements of the ^{238}U(n, γ) cross section at thermal and fast neutron energies. Nucl. Sci. Eng. 78, 239.

Poppe, C.H., Anderson, J.D., Davis, J.C., Grimes, S.M., Wong, C., 1976. Cross sections for the ^{7}Li(p, n)^{7}Be reaction between 4.2 and 26 MeV. Phys. Rev. C 14, 438–445.

Pronyaev V.G., 1999. Summary report of the consultants meeting on assessment of nuclear data needs for thorium and other advanced cycles. INDC (NDS)-408, International Atomic Energy Agency, Vienna.

Quang, E., Knoll, G.F., 1992. Absolute measurements of the fast neutron capture cross section of ^{238}U. Nucl. Sci. Eng. 110, 282.

Shani, G., 1983. (n, 2n) Cross-section measurement of ^{93}Nb, ^{197}Au and ^{238}U with fission-neutron spectrum and its dependence on the asymmetry term. Ann. Nucl. Energy 10, 473.

Shibata, K. et al., 2011. JENDL-4.0: a new library for nuclear science and engineering. J. Nucl. Sci. Technol. 48 (1), 1–30.

Tan Vuong H., Hai Nguyen C., Hiep Nguyen T., 1996. Measurement of capture cross sections of 238U on the filtered keV-neutron beams. INDC (VN) – 008.

Voignier, J., Joly, S., Grenier, G., 1992. Capture cross sections and gamma-ray spectra from the interaction of 0.5- to 3.0-MeV neutrons with nuclei in the mass range A = 45 to 238. Nucl. Sci. Eng. 112, 87.

Wang, X., Jiang, S., He, M., Dong, K., Xiao, C., 2010. Nucl. Instr. Meth. Phys. Res. A 621, 326.

Wisshak, K., Kappeler, F., 1978. Neutron capture cross-section ratios of ^{240}Pu, ^{242}Pu, ^{238}U, and ^{197}Au in the energy range from 10 to 90 keV. Nucl. Sci. Eng. 66, 363.

Ziegler J.F., Zeiler M.D., Biersack J.P., 2008. SRIM-2008.04. <http://www.srim.org/>.